Studies of a veto system for the Braidwood reactor neutrino experiment

Veto Working Group*

(Dated: May 19, 2005)

Abstract

This report summarizes several studies of the design of a veto system for the Braidwood experiment. We have studied two idealized designs for the Braidwood veto system and find both will meet our goal of fewer than one fast neutron background event per day per detector. We have developed software tools which will be used to show we can track muons with sufficient accuracy to measure backgrounds from neutrons and spallation isotopes in the neutrino detector. Consideration of several realistic designs indicates the practical requirements of the system can likely be met for costs outlined in the project description. Finally, we discuss the opportunity of detecting supernovea using a scintillator-based veto system.

PACS numbers:

*Electronic address:

I. GOALS AND REQUIREMENTS

Three primary requirements drive the design of the veto system [1]:

1. Active detectors must identify cosmic ray muons which could produce neutron background in the fiducial region of the neutrino detector.

2. Neutrons produced by muons which do not trigger the active detectors must be absorbed before they reach the neutrino detector. The shield must also absorb all gamma ray photons emitted by the surrounding rock.

3. The muon identification must allow *in situ* determination of the neutron and isotope background rates.

The veto system consists of two major components: active detectors and passive absorbing material. For the purposes of this study, we consider two basic designs, shown in Fig. 1. The passive design consists of 1 meter of heavy concrete absorber with two or more layers of position sensitive detectors mounted on the outer (and possibly inner) surfaces. The active design consists of 2 meter thick tanks containing water or scintillator viewed by photo-tubes with 3% photo-cathode coverage. In each case, the system is a simple box surrounding the neutrino detector. We have calculated the expected neutron background at 300 and 450 MWE for both systems and we believe we have shown that both systems will reduce the neutron background to fewer than one neutron induced background event per day per detector.

In addition, we have identified the following requirements stemming from the location and construction of the detector:

- **Modularity** - in order to reduce tunneling costs, the access shafts need to be as small as possible. Given that we want to move the steel vessel into position while it is full, the shaft will be at least 8 m in diameter. This requires each module to fit down an 8 m diameter shaft.

- **Access to neck** - calibration sources will need to go down the neck into the fiducial region. We take as a requirement that the veto system will need to allow access to the neck with a minimum of time for dismounting of the veto system at the neck. In

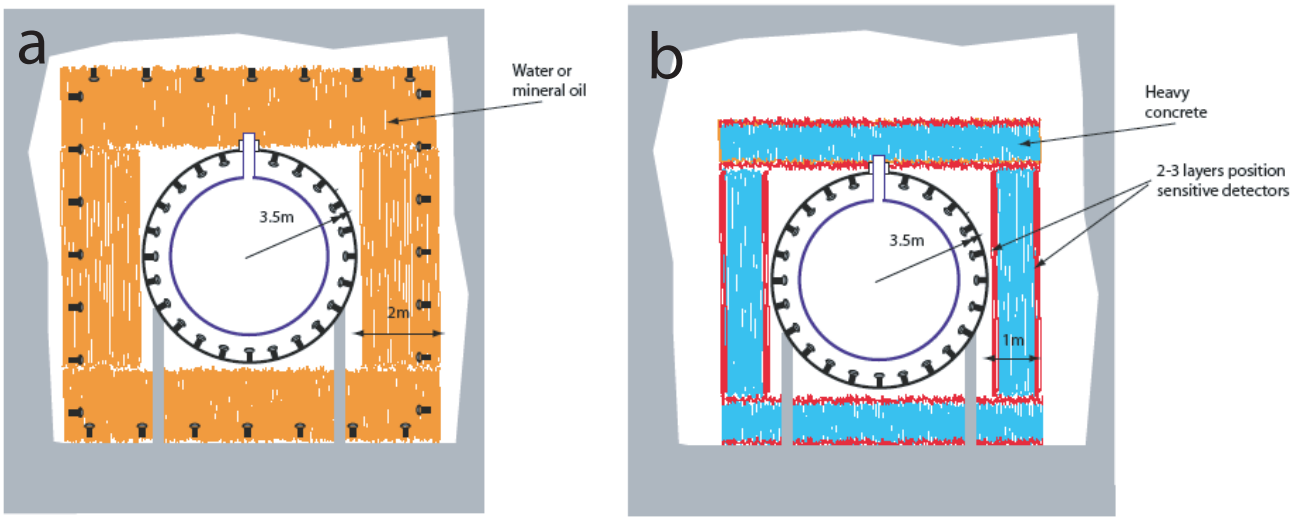

FIG. 1: a) Baseline active shielding design. The photo-cathode coverage is 3% inside the tanks, which contain water or mineral oil. b) Passive design using 1 m heavy concrete. Position sensitive detectors mount in the outside (and possibly the inside) of the shield.

addition, there will need to be space around and above the neck for access. We may also need to access the buffer region of the neutrino detector for calibration.

- **Moving of the neutrino detector** - we plan to move the neutrino detector for cross calibration, which means we will have to be able to get the veto system apart to move the neutrino detector.

In our report, Section II summarizes the background calculations and Section III gives some first ideas for more optimized systems. Section IV describes some additional physics opportunities with the veto system.

II. BACKGROUND CALCULATIONS

Fig. 2 shows how neutrons enter the neutrino detector and cause neutrino background events. There are two ways: first, a muon may produce a neutron in the surrounding rock without triggering the veto system and the neutron then penetrates the shield. Once inside the fiducial volume, the neutron hits a proton, causing it to recoil with sufficient energy to make enough scintillation light to mimic a positron. The neutron then captures on gadolid-

ium, completing the time coincidence. In a second mechanism, the muon produces a neutron and passes through the veto without making a trigger. We compute the background from both cases below, assuming a veto efficiency of 98%. We have used MARS[2], GEANT4[3] and FLUKA [4] to estimate the neutron background at the surface of the vessel. The neutrons are created by muon spallation interactions in the rock and veto material. The neutrons of concern typically emerge with 10-200 MeV of energy and propagate through the material in which they were produced, Fig. 3. We use the incident muon energy and zenith angle spectra computed using GEANT4 by Pilcher and Hurwitz[5] at 300 and 450 MWE as a starting point. While the production of neutrons by muon spallation is well simulated, the transport of neutrons with energies above 20 MeV remains rather uncertain due to lack of data. Table I shows comparison of codes with data for neutron interaction in carbon. We include the spread of these different calculations in our estimation of the uncertainty of the neutron background.

A. Neutron propagation comparisons

A basic test of the neutron Monte Carlo codes was made by comparing the energy distribution of neutrons that survive passage through 10cm of material. If the incident neutron survived with greater than 99.2% of its initial energy, that is equivalent to a total cross section measurement. If the outgoing energy is larger than 75% of the original energy, that is equivalent to a measurement of the total nonelastic cross section. Comparisons were made with respect to existing total cross section data and a NASA parameterization of the nonelastic cross section [6]. In the Table I, we show the results for MARS, FLUKA, and GEANT4 relative to the exisitng data and parameterization. Carbon has the best data, so that element is chosen for comparisons. Although the carbon cross section has resonant structure, the data is smooth for 5-10 MeV neutrons. Ongoing problems in the interpretation of the FLUKA results prevent a comparison at the lower energies.

The total cross section is well-produced at each energy with the exception of GEANT4 at 50 MeV. Given the estimated error of $\pm 20\%$ in the nonelastic cross section, agreement is acceptable. Investigation into the cross section database used for each Monte Carlo is ongoing.

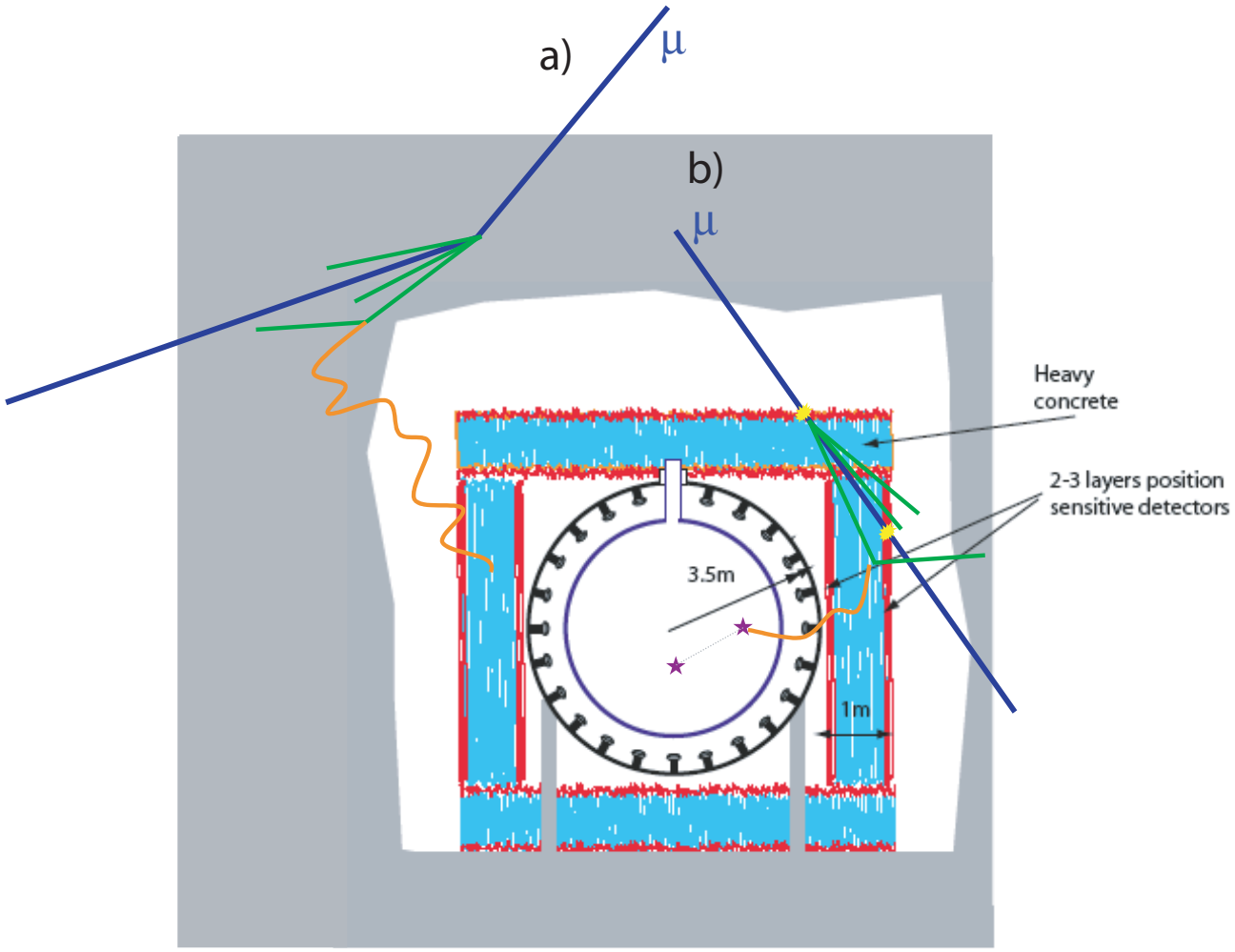

FIG. 2: Two mechanisms for neutron production. Track a) shows neutrons produced in the surrounding rock, which are absorbed by the shielding. Track b) shows neutrons produced in the shielding close to the neutrino detector which are tagged by the veto system.

B. Calculation using MARS

A first calculation using MARS considers neutrons produced in the rock surrounding the shielding and those produced inside the shielding separately. For neutrons produced in the outside rock, a convolution of the Pilcher-Hurwitz muon energy spectrum with the neutron energy spectrum from muons as a function energy given in [7] gives the neutron energy spectrum and a production rate of 177 neutrons/ton/day. For the neutron transport in the rock, we simulate neutron attenuation in a 2 m thick infinite slab of rock. Neutron survival

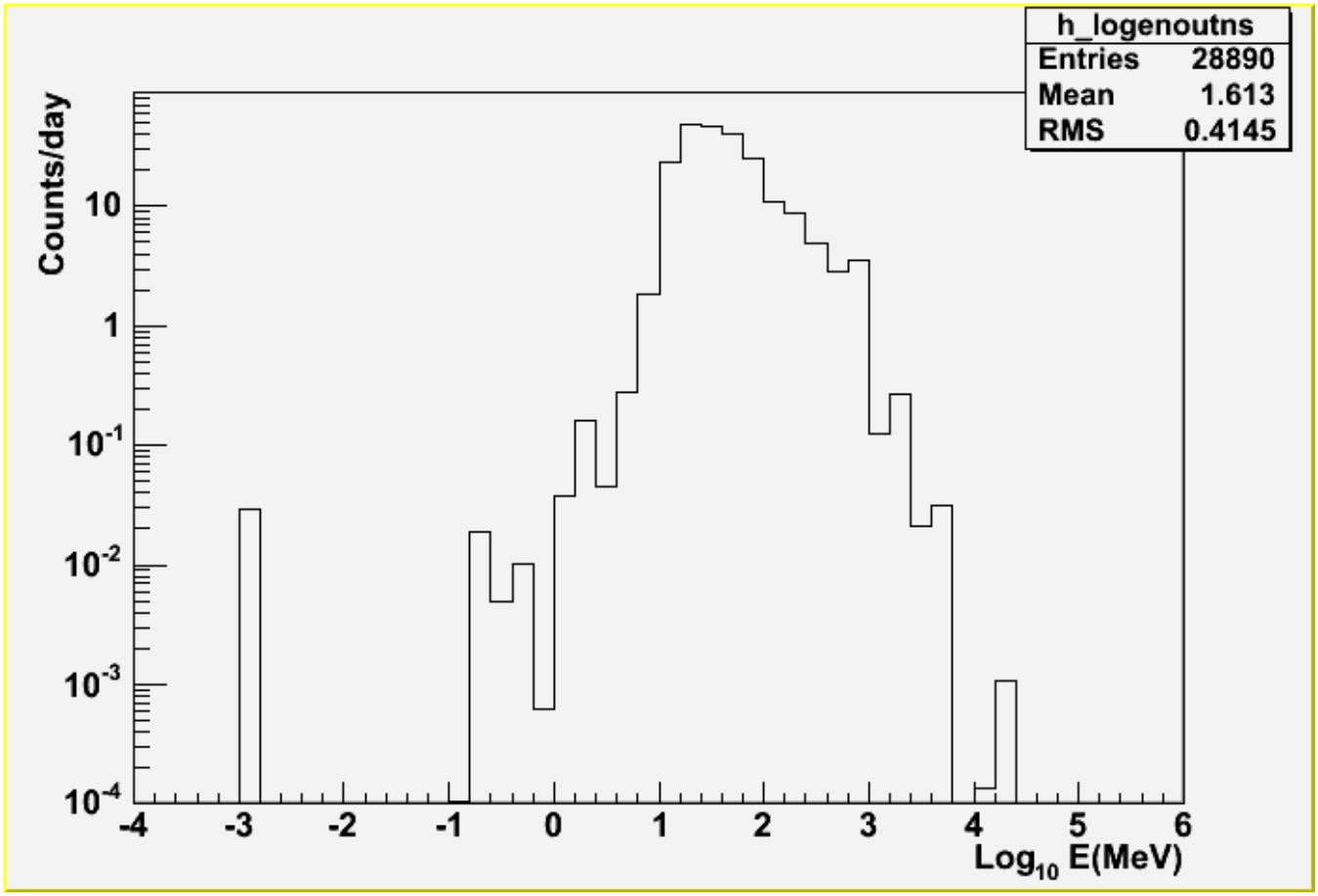

FIG. 3: Energy spectrum of neutrons emerging from the rock surrounding the detector system

rates in 10 cm steps are used to compute the neutron flux at the inner surface of the rock. We find 2100 neutrons/day emerging from the rock and directed toward the detector volume. These come from the first 20 cm of rock and have an energy spectrum similar to that at production. Next, the 1m heavy concrete shield and 0.5 m mineral oil layer are modeled and we find that less than 1% of neutrons survive. We also look at the detector response to the prompt energy deposition (not including neutron capture) and calculate the fraction of surviving neutrons that have a prompt visible energy in the reactor neutrino range (0.8 to 8 MeV) to be about 20%.

The parent muons for many of these neutrons may at some point pass through the veto detectors and be tagged. Assuming only the parent muon angular distribution and the distance that a neutron was produced from the veto, we estimate 88% of neutrons produced in the surrounding rock which can reach the fiducial volume would be accompanied by a

σ_{total}				
n KE (MeV)	data	Ratio to data		
	(barns)	MARS	FLUKA	GEANT4
5	1.237±.011	1.01		1.10
10	1.19±0.04	1.00		0.93
50	0.953±.002	1.00	1.08	0.66
100	0.491±.002	0.97	1.01	0.90
$\sigma_{nonelas}$				
n KE (MeV)	NASA	Ratio to NASA		
	[6]	MARS	FLUKA	GEANT4
5	0.424	1.47		1.82
10	0.621	1.18		1.27
50	0.313	0.90	1.32	1.18
100	0.222	0.86	1.23	1.21

TABLE I: Upper table shows the ratio of the effective total cross section for carbon based on various Monte Carlo calculations to the tabulated value from the BNL archive. The reference data is also given. Lower table shows the ratio of the effective nonelastic cross section to the value from the NASA parameterization. The estimated error of the parameterization is about ±20%.

veto tag.

Calculation of the background from neutrons produced in the shield region proceeds in a similar way. Survival factors for neutrons produced both inside and outside the shield are given in Table II. With a 99% efficient veto detector system we expect less than one fast neutron background per detector per day.

A simple hand calculation cross checks part of this result: the number of neutrons emerging from the surface of a 3.5 m radius spherical cavity in the rock may be calculated analytically. For energies above 10 MeV, MARS gives a neutron attenuation length in dolomite of 24 cm. Using a muon flux of $0.2/m^2 - s$ and average muon energy of 84 GeV form Pilcher and Hurwitz, we find 4,500 neutrons/day emerging from the surface of the cavity, which compares well with the 4,100 used in the study above.

Sample	Neutrons Produced	
	Inside Shield	Outside Shield
Initial Neutrons (/detector/day)	2000	2100
μ Not Tagged in Veto	1%	12%
Attenuation in Shielding and Buffer Oil	18%	0.93%
Positron-like Prompt Visible Energy	27%	20%
μ Not Tagged in Inner Detector	26%	
Surviving Neutrons (/detector/day)	0.25	0.47

TABLE II: The neutron background survival factors for each step of the analysis for neutrons produced outside the shield and surviving to the inner edge of the rock and for neutrons produced inside the shield and surviving to the inner edge of the shielding.

C. Calculation using GEANT4

A full GEANT4 simulation provides an independent approach. Since GEANT4 and FLUKA have been compared in detail and found in rough agreement [8] and FLUKA compares well with available data. The GEANT4 simulation proceeds in two passes, both using the same detector geometry. In the first pass, muons sampled from a logarithmically flat energy distribution over the range 1-1000 GeV and a flat zenith angle distribution over the range $\cos\theta_z$=-1 to -0.3 start in one of six 4×4 m patches shown in Fig. 4. The muons and any secondaries except neutrons propagate through the rock and detector system. We record all energy depositions in sensitive detector volumes. When a neutron is produced, its position and momentum are recorded for use in the next pass. For the passive shielding design, we assume an event is vetoed if the active detectors record at least one minimum ionizing particle passing through the 10 cm thick detectors. For the active shielding design we assume the equivalent of 10 photo-electrons in a photo- multiplier system.

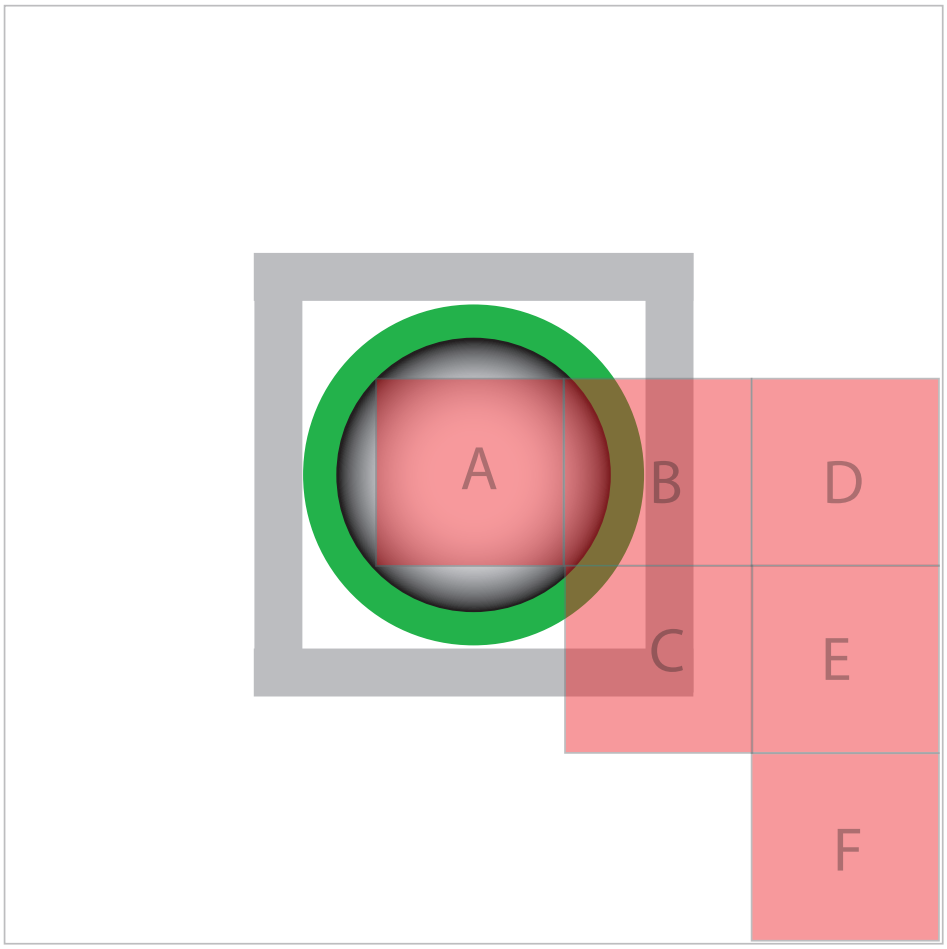

FIG. 4: 4×4 m sampling patches over the top of the detector. Patch A receives a weight of one, patches B, D, E and F have weights of 4 and C has a weight of 8. This allows sampling a large region of rock around the detector.

Fig. 5 shows how the veto system works: for a fully efficient veto system, a muon interaction which produces a neutron within 6 m from the center of the neturino detector result in a veto. The shielding then absorbs enough neutrons produced at larger radii to keep the background rate below the required 1/day. For a 2 m thick active system, the keepout zone is 7.3 m.

In the second pass, each neutron is considered as a point source and we compute a weight for that neutron to arrive at the surface of the vessel with a kinetic energy K' based on its position, direction of travel and initial kinetic energy K. A second weight, based on

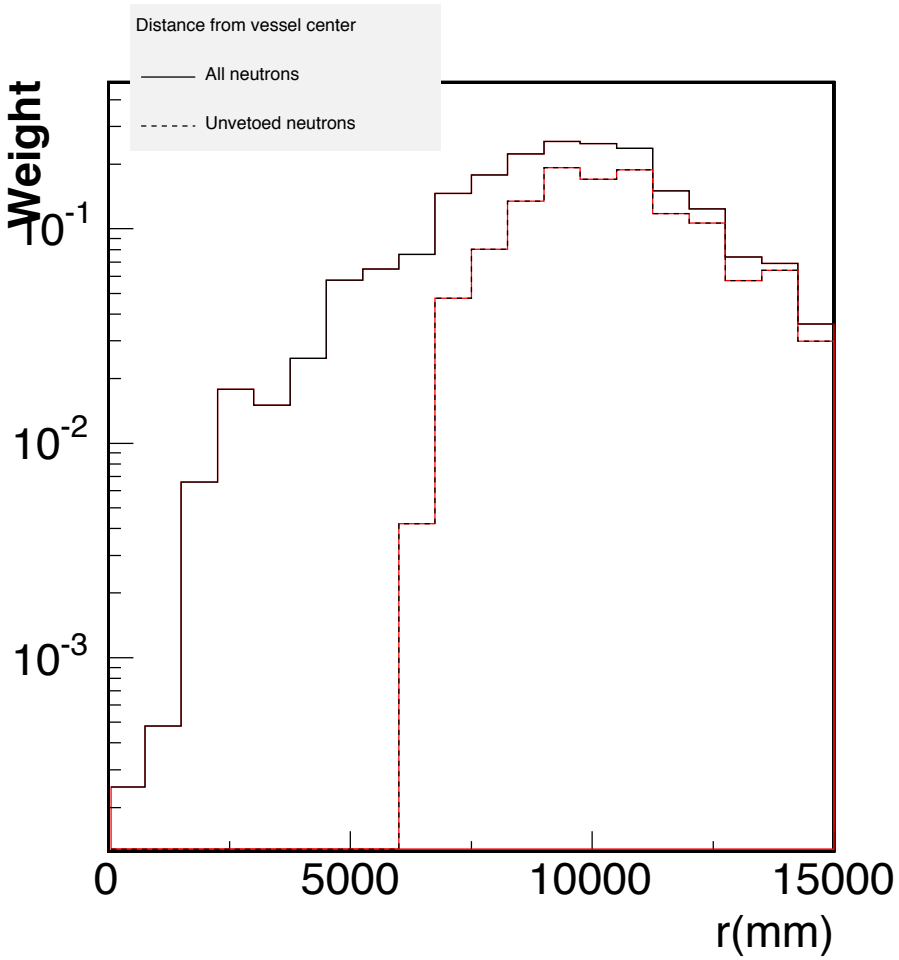

FIG. 5: Red curve shows the radial distribution for all neutrons, green curve shows those neutrons which do not trigger the veto.

the Pilcher-Hurwitz spectrum is applied to take into account the production probability of the parent muon and the probability of starting in a given patch. The weighting method allows us to run the simulation once and then re-weight for any depth. We have two points of comparison with the previous calculation: we find a rate of 167 neutrons/ton-day in the rock (to be compared with 177/ton-day for the previous calculation) and 4,700 neutrons/day emerging from the inner surface of the detector cavity (compare with 4,100 for the MARS calculation and 4,500 for the hand calculation).

The full simulation works only until the surface of the steel vessel. At that point, the neutron energy, position and momenta are recorded and used in the inner detector simulation,

Depth (MWE)	Neutron production rate in rock (n/ton-day)	Unvetoed neutron rate at vessel (n/day)	Background event rate (n/day)
300	360	3	0.3
450	167	1.5	0.2

TABLE III:

GEANT4 neutron simulation results for passive detector design. Rates for the active design are similar.

to find the fraction of neutrons which produce neutrino background events in the detector. We currently estimate 10% of the neutrons arriving at the vessel produce background events. The total rates at 300 and 450 MWE are summarized in Table III.

In summary, we have carried out two independent studies of the veto system and find the performance of our baseline passive system meets our goal. The studies agree at the 20% level for the neutron production in the rock (which compares the muon interaction models) and the neutron flux inside the cavern (which compares neutron transport models). The final results agree to within a factor of two, which we find reasonable given the differences in the neutron transport.

III. DESIGN OPTIONS

Our simulations show the designs in Fig. 1 fulfill our background reduction requirements. We have begun considering optimized designs which meet the practical requirements of cost and technical feasibility. In the course of our study, several options have arisen which are discussed below.

A. Passive shielding

Concrete is a simple substance to work with. For shielding purposes, heavier elements are often added. We found a concrete mix that has a little over half its weight in iron. It has been successfully used by the CHESS collaboration at Cornell Electron Storage Ring (CESR). We find that the neutron attentuation of heavy concrete has a significant advantage

over regular concrete of the same thickness, particularly for low energy neutrons. We've been investigating two ways to use 1 m of heavy concrete.

The box design, Fig. 6, follows from our baseline passive design and consists of 1 m of CHESS concrete instrumented with large proportional tubes or resistive plate chambers (RPCs) on the outer surface. Detectors completely cover the outside surface, allowing for tracking of muons that transit the inner detector. The top and side panels mount on a movable base which straddles the neutrino detector. The front and back panels move separately and access to the neck is obtained by moving the front panel back. This gives the best access to the inside of any of the designs. Each panel is of modular construction, consisting of about $4m \times 2m$ assemblies. Each assembly consists of the concrete shielding material with the detector elements mounted on the side. This allows the assembly and testing of each module on the surface. Integration of each panel would take place underground. The active part of the detector would be two or three layers of RPC's, or large proportional tubes. Using segmentation of roughly 30cm, we obtain a good compromise between tracking resolution into the fiducial volume and readout cost.

The quonset hut design, Fig. 7 follows many of the ideas of the box design, but reduces the volume occupied by the detector assembly. This would result in a savings in both area and weight, lowering costs of excavation, shielding, and readout. It would also take advantage of the strengths inherent in an arch. Like the box design, the central assembly covers the top and sides of the neutrino detector.

B. Active shield

The "silo" configuration, Fig. 8, consists of a four piece cylindrical lower portion and a four piece hemispherical top. A cylindrical piece provides shielding below the steel vessel. Each component is small enough to be moved through an eight meter diameter access shaft. The shield is two meters thick in all dimensions. The water in the tanks are viewed by photo-tubes.

Access to the neck is provided by a hole in the top; the neck of the acrylic vessel extends all the way through the shield. When not needed for deploying sources, the neck is sealed by inserting a fixture, Fig. 8. The neck fixture consists of two disks of close to the size of the neck. The lower is made of acrylic and serves to complete the acrylic sphere. The upper

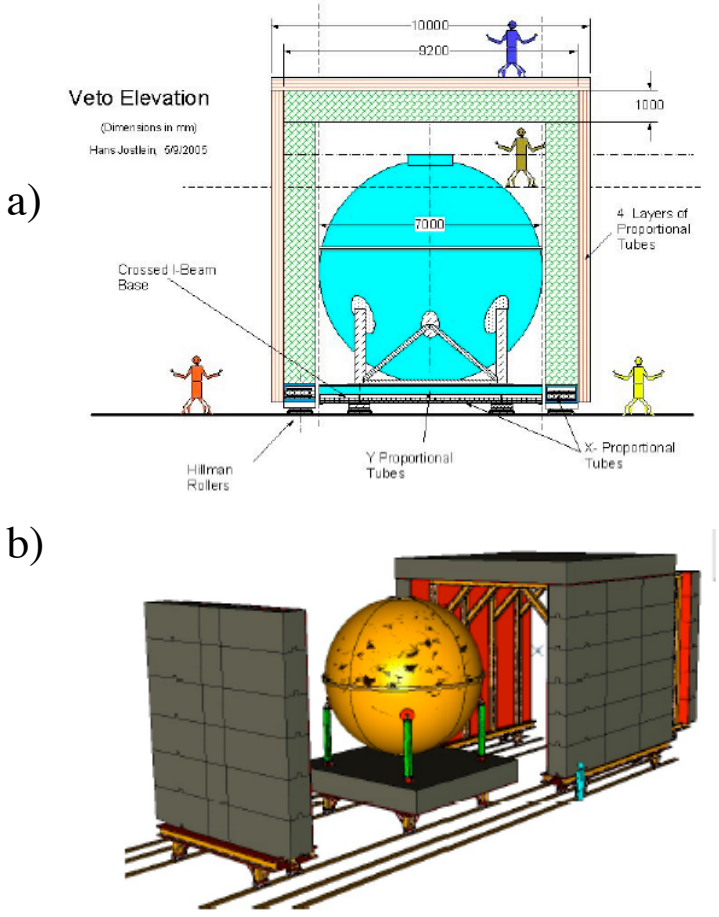

FIG. 6: Design for a passive detector using modular boxes. The outer and (optionally) inner surfaces of the shielding are covered with detectors (RPC's, wire chambers or scintillator panels.)

disk is located at the radius of the steel vessel and is opaque in order to optically separate the portion above the steel vessel. Photo-tubes view both regions.

C. Configuration comparisons

We conclude with a comparison in Table IV. A preliminary estimate of the costs show no show-stoppers for any one design, although the total costs do vary. Groups within the

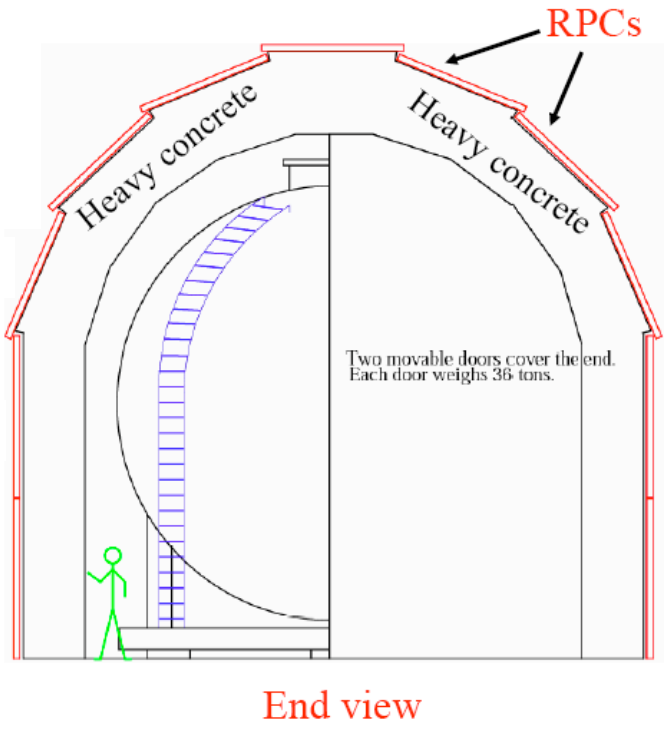

FIG. 7: Quonset hut design end view. Instrumented doors on the front and back move away to allow access.

Braidwood collaboration currently pursue studies of different detector technologies.

IV. PHYSICS OPPORTUNITIES WITH THE VETO SYSTEM

One of the proposed designs for the Braidwood veto shields involves the use of a modular, 1-2 meter-thick water Cherenkov detector. This would constitute a sizable bulk of between 0.3 and 0.7 kilotons of liquid per detector. We have explored what could be done with the shield itself were we to use a gadolinium loaded scintillator mixture for the liquid instead of water. Chief among these would be their use as a sensitive supernova detector which could rival KamLAND and provide a long-term future for the Braidwood facility beyond the reactor measurement itself. Due to the geographic location of Braidwood with respect to Japan, it might even conceivably allow a direct measurement of earth matter effects. A study of the event rates shows the veto would detect several hundered neutrino events for

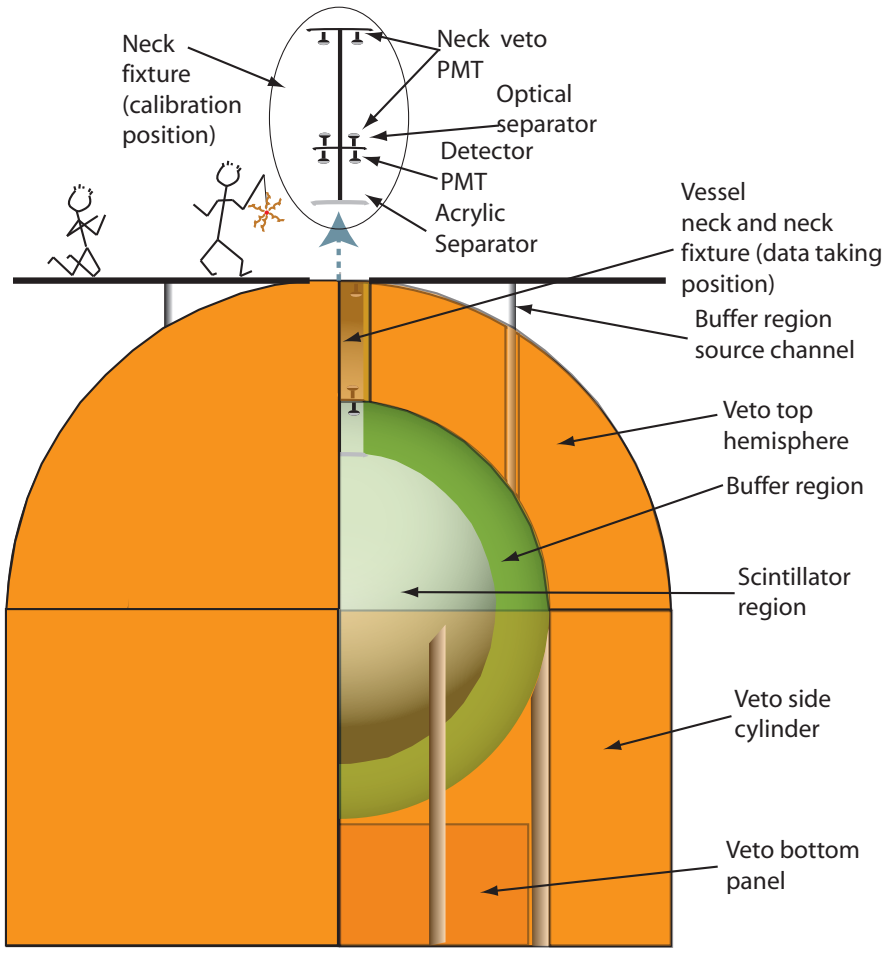

FIG. 8: "Silo" veto system using nine tanks containing either liquid scintillator or water with photo-tubes mounted in the inside. The system provides 2 m of shielding in all directions, but could be reduced in thickness to 1m.

a supernova 10 kpc distant giving additional information about the mass heirarchy and θ_{13}. A full description is given in [9].

V. SUMMARY

We have carried extensive preliminary studies of the performance of passive and active veto systems using two independent methods and find in both cases, the baseline designs meet our requirments. Consideration of practical designs show there are several options which could be built within our proposed budget. A final design choice awaits further study.

	Shield (g/cm^2)	Mass (kt)	Surface area (m^2)	Detector	Channel Count
Box	1 m concrete (350)	1.94	503	Prop. tube	1944
	1 m concrete (350)	1.72	460	RPC	5751
Quonset	1 m concrete (350)	1.46	379	RPC	4740
Silo	2 m water (200)	0.72	457	PMT	300
	2 m minreal oil (200)	0.72	457	PMT	300

TABLE IV: Comparison of system design options. RPC refers to resistive plate chambers, PMT refers to photo-multiplier tubes.

Finally, a scintillator based veto presents an interesting possibility for detecting supernovea.

---

[1] Project Description, http://mwtheta13.uchicago.edu, 2005.

[2] N.V. Mokhov, et al., Fermilab-FN-628, 1995.

[3] Geant4 Collaboration, NIM A506(2003)250.

[4] P. Aarnio et al., CERN/TIS-RP/93-10, 1993.

[5] J. Pilcher and M. Hurwitz, http://mwtheta13.uchicago.edu, 2005.

[6] R.K. Tripathi et al., NASA Technical Paper 3656, 1997.

[7] Y-F Wang et al., hep-ex/010149.

[8] H.M. Araujo et al., hep-ex/0411026.

[9] S. Biller, http://mwtheta13.uchicago.edu, 2005.